

Performance test of the new dE/dx counter in the DIRAC beam line

Received May 24, 2013

Soichiro AOGAKI¹⁾

Masami CHIBA²⁾

Kenji OKADA¹⁾

Fujio TAKEUTCHI¹⁾

¹⁾ Kyoto Sangyo University

²⁾ Tokyo Metropolitan University

Abstract

A new dE/dx counter to be used in an intense beam was designed for the DIRAC experiment. A performance test was carried out by placing the counter in the DIRAC spectrometer. Very good counting efficiency and time resolution were observed. In parallel, a performance test was carried out using the cosmic ray. The latter result is reported in a separate paper.

Keywords: DIRAC experiment, $\pi^+\pi^-$ atom, ionization hodoscope, PSPM, fiber light guide

1. Introduction

A new counter is needed to replace the existing dE/dx counter (IH) whose counting efficiency is not good enough. Also, as a counter placed in the front-end, its performance limits the increase of the primary beam intensity in DIRAC experiment [1], while other detectors could accept a more intense beam. The DIRAC experiment is seeking for pairs of particles with a very small distance at the front-end detector level. The candidate pairs are picked up by SFD (scintillating-fiber detector) which has at the same time a good spatial resolution and a moderately good time resolution. But when the pair of minimum-ionizing particles are geometrically very close, they look like a single hit for SFD. The primary role of IH is to tell either the seemingly single hit contains really two particles or a real single hit by measuring their (its) energy loss in

the counter.

The inadequacy of the current IH comes from the high beam intensity including background particles. It was therefore necessary to build a new counter which can provide with a precise pulse-height information and still can accept a beam intensity of about $3 \times 10^7/s$ on a $10 \times 10 \text{ cm}^2$ plane.

Hereafter, this new dE/dx counter (new IH) tested is designated as the counter in this article.

2. Construction

A way to improve the efficiency of IH is to increase its granularity. In the new design, the number of slabs within the width of about 10 cm is increased from 16 to 32. From the recovery time point of view, PMT Hamamatsu H6568 Mod III was chosen as the photo device. The dimension of a slab is of 3.5 mm wide and 122 mm long. Its thickness is limited to 2 mm in order to keep the multiple scattering effect small. Therefore the attenuation of the light within a thin and long slab becomes non-negligible which is harmful to the uniformity of light output independent of hit position. The problem of the non-uniformity of the light output was solved by reading-out the light from two ends of the slabs.

As it is very difficult to design 64 solid light guides to connect the slabs to the photocathodes of the PMT, KURARAY 0.5 mm ϕ multi-clad clear fiber was chosen for the light guide. This makes the construction easier, but a certain loss of light at the joint of the fiber and the slabs is unavoidable. In the preliminary test [2], it was found that at least a thickness of 2 mm for the slabs was necessary to produce some 20 photoelectrons as the pulse height, in a passage of a minimum-ionizing particle, even with the PMT chosen equipped with the new ultra bialkali photocathode.

To minimize the Landau effect, 4 layers of planes were built for the counter. Two planes whose 32 slabs are arranged vertically are called X and X' planes, while two planes with horizontal slabs are called Y and Y' planes. The detail of the construction of the counter is reported in [3].

3. Performance test

As the counter has been designed to be used in high-intensity beams, it is desirable to perform a test to investigate the performance of the counter in such a beam. However, no such beam was available at the time of the test, thus it was carried out in the DIRAC beam line (T8) of PS at CERN.

The counter was placed after the HH (horizontal hodoscope) of the positive arm of the DIRAC spectrometer. The counting rate at that point of the spectrometer was about $7 \times 10^5/s$.

Dedicated F1-TDC-ADC units [4] have been used to read-out the signals from the counter. One unit can read out 16 channels (8 slabs) of signals. Therefore one needs 16 units to read out the whole counter. But only 6 units were available at the time of the test. Thus only 3 (half) planes were read-out at a time. By changing the configurations 4 times, we checked the performance of all the planes.

It was found that all the planes worked equally well. In this report, however, we describe mainly the test results of the first configuration, where two vertical (half) planes, X and X' and one horizontal Y plane were read out. Although each plane contains 32 slabs, only the first half (16 slabs) have been read out in this configuration.

4. Results

4.1 Light output (number of photoelectrons) and its uniformity

Fig. 1 shows a typical pulse-height distribution for the tested planes in the first configuration. The particles recorded are mostly minimum-ionizing particles, mostly positive pions, but also contain up to 11 % of positrons.

The F1-TDC-ADC does not show pedestal peaks. The reason is that when the charge is zero, no output signal is produced. However, this PMT (H6568 Mod III) produces cross talks of about one photoelectron between 16 channels at the level of photochathode [5]. In addition

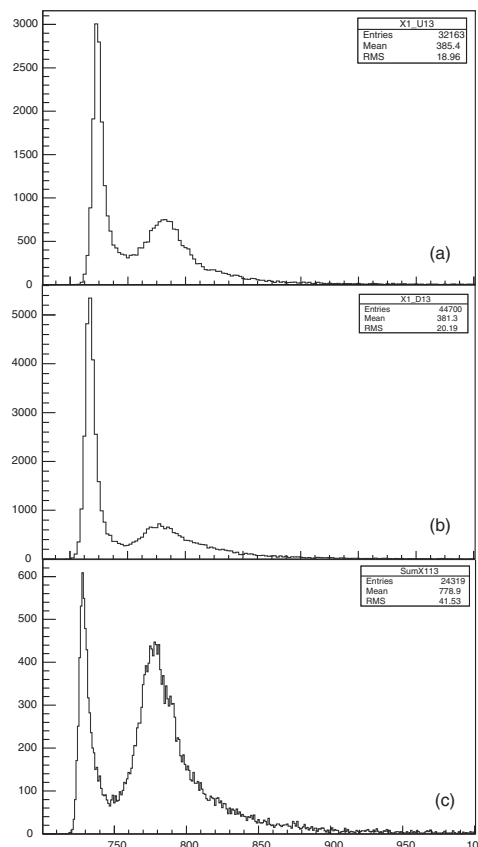


Fig. 1 Typical light output from a slab is shown. The left-side peak is due to the cross talks (see text). The lower side of this peak is cut by the threshold set to the F1 unit (10mV). The right-side peak is due to the passage of minimum-ionizing particles in the scintillator slab of 2 mm thick. (a) Output to one end of the slab. (b) Output to the other end of the slab. (c) The outputs from the two ends are added in order to reduce the attenuation effect. The units on the coordinate is F1-TDC-ADC channels.

there is a cross-talk in the light guide of the counter up to the level of a few photoelectrons [3]. In Fig. 1a a typical light output from one end of a slab is shown. The left-side peak is due to these cross talks. The lower side of this peak is cut by the hardware threshold set to the F1 unit (10 mV), thus the peak is not exactly at one photoelectron.

The right-side peak is due to the passage of minimum-ionizing particles in the scintillator slab of 2 mm thick. Although the pulse-height calibration has been performed many times during the data acquisition, the information about the zero-point of the F1-TDC-ADC is not easily available. Therefore it is difficult to estimate the absolute number of photoelectrons corresponding to the right-side peak in this measurement. A separate test using traditional ADCs and cosmic rays shows that the peak corresponds to more than 20 photoelectrons [3].

To minimize the effect of the light attenuation in a slab, signals from two ends were added. The result is shown in Fig. 1c. This reduces as expected the attenuation effect, and one can observe that the peaks become narrower compared to Fig. 1a and Fig. 1b which show the light output from the opposite side of the same slab.

Fig. 2 shows a typical pulse-height distribution (signals from both ends are added like in Fig. 1c) when only electron-positron (e^+e^-) trigger was chosen. The peaks seem to be slightly narrower with this trigger. Despite the fact that the energy loss could be better defined for the pions than for positrons, this could be explained by the fact that the divergence of the tracks of the positrons at the location of the counter is smaller (the variation of the angle of the incoming particles with respect to the normal to the plane is smaller) than that of the pions.

DIRAC spectrometer can tell the position of the particles hitting the counter. By using this feature, we try to select events by applying a cut (window) to the hit position of the tracks. Fig. 3a, 3b, 3c. show two-dimensional displays of the calculated positions of the events not detected by (which missed) X, X', and Y planes. The white "shadows" indicate the location of the instrumented slabs whose size is 12.2 cm \times 5.6 cm. The borders of the shadows, however, are blurred. This is due to the fact that the prediction of the track position by the spectrometer using the offline analysis program Ariane [7] contains errors.

To evaluate the errors, the distribution of the predicted position of the particles recorded by each slab of the counter is shown as a box plot for each plane in Fig. 4. From this, the error in the

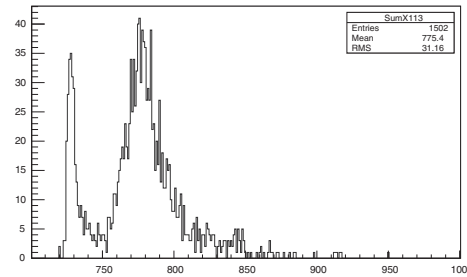


Fig. 2 Same as Fig. 1, but only events with e^+e^- trigger are recorded.

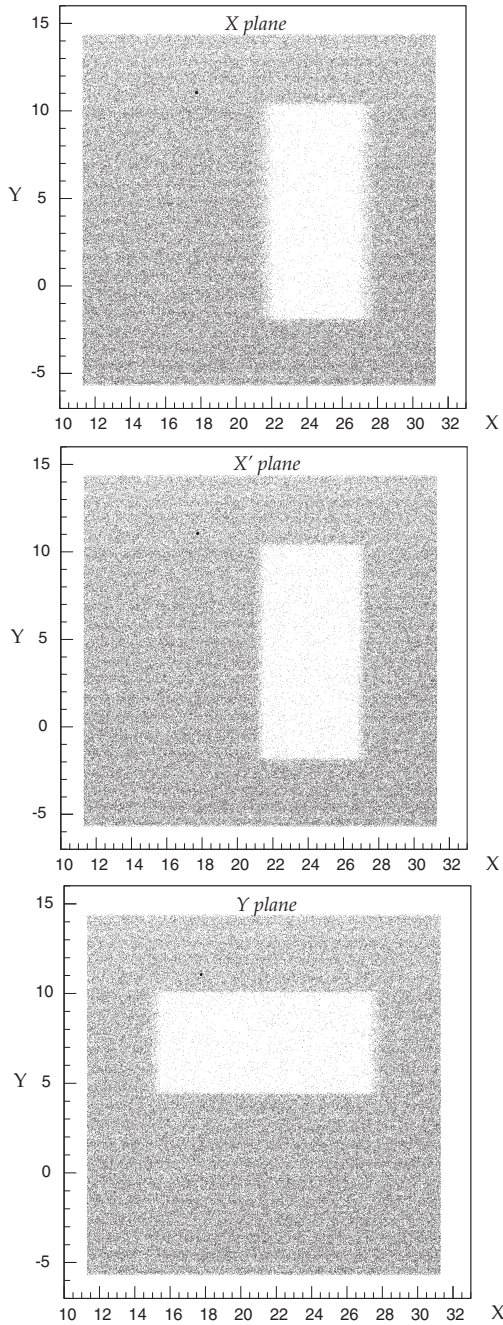


Fig. 3 Events not detected by X (top), X' (middle), and Y (bottom) planes are shown in 2-dimensional scattered plots. The units on the two axes are cm.

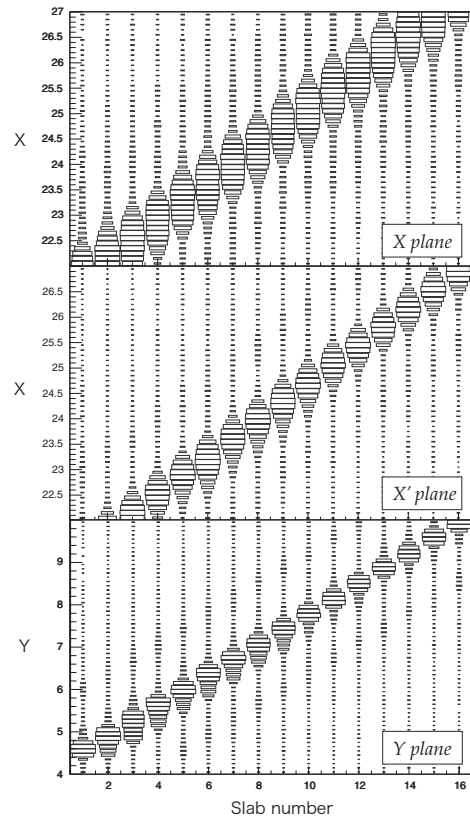


Fig. 4 Distributions of the predicted position (unit: cm) of the particles recorded by each slab of the counter, shown in box plots. The positions of the slabs are precisely known. Top: X plane, Middle: X' plane, and Bottom: Y plane. From this graph, the error in the DIRAC spectrometer (Ariane) prediction is estimated to be 18.5 mm in horizontal and 12.0 mm in vertical direction.

prediction is estimated to be 18.5 mm in horizontal and 12.0 mm in vertical directions.

The real size of the overlapped region of X, X' and Y planes is 5.43 cm \times 5.6 cm. But taking these uncertainties in consideration, we chose the size of the above-mentioned window to be 3.58 cm wide (22.71 cm – 26.29 cm) in the horizontal (X) direction and 4.40 cm tall (5.05 cm – 9.45 cm) in the vertical direction (Y) such that particles falling inside of the window surely hit the counter. The position of the window with respect to the overlapped image of the “shadows” is shown in Fig. 5. The particles going through the window are called candidate particles.

4.2 Timing resolution

The timing of each hit on the counter is recorded using the F1-TDC-ADC. The timing of the particle hitting VH (vertical hodoscope) of the spectrometer, as well as the speed of the particle is known with a high precision. (RMS 113 ps [6]) The correlation between the timing of the hit recorded on the detector and that of VH is shown in Fig. 6 as a dot plot. In this analysis, the timing of a hit on a slab is defined by the average of the timing of two ends of the slab.

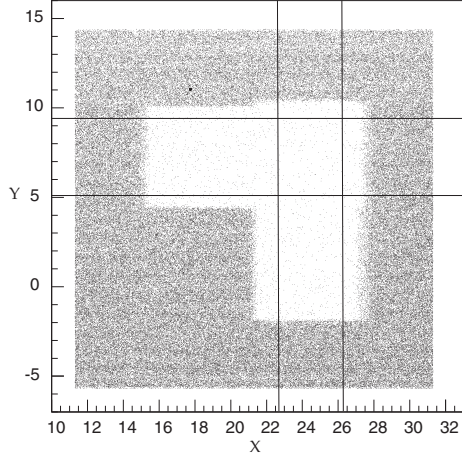


Fig. 5 The definition of the window (X and Y directions) is shown in this 2 dimensional display. We chose the size of the window (horizontal: 22.71 – 26.29 cm, vertical 5.05 – 9.45 cm) such that particles falling inside of the window surely hit the counter with the precision of the spectrometer is considered. The units on both axes are cm.

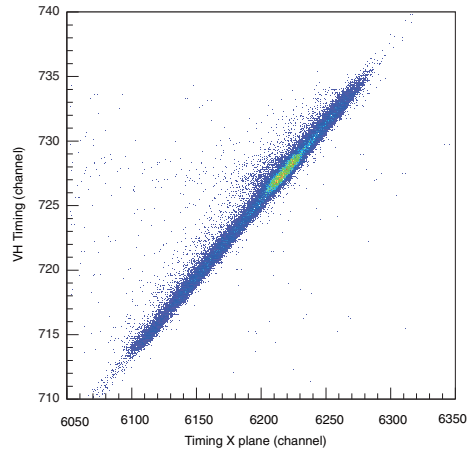


Fig. 6 The correlation between the timing recorded by VH of the spectrometer and the timing recorded by the detector X plane is shown as a dot plot. Similar plots can be obtained for X' and Y planes. The units on both axes are channels.

Fig. 7 shows the distribution of the timing recorded by X, X' and Y planes. By fitting the peaks with a Gaussian, the width of the peaks are found as shown in Table 1.

Table 1 Evaluated timing resolution of all the events using VH timing

plane	width (RMS) of the timing peak	width after removal of the VH width
X	331.7 ps	311.1 ps
X'	309.1 ps	287.7 ps
Y	323.2 ps	302.8 ps

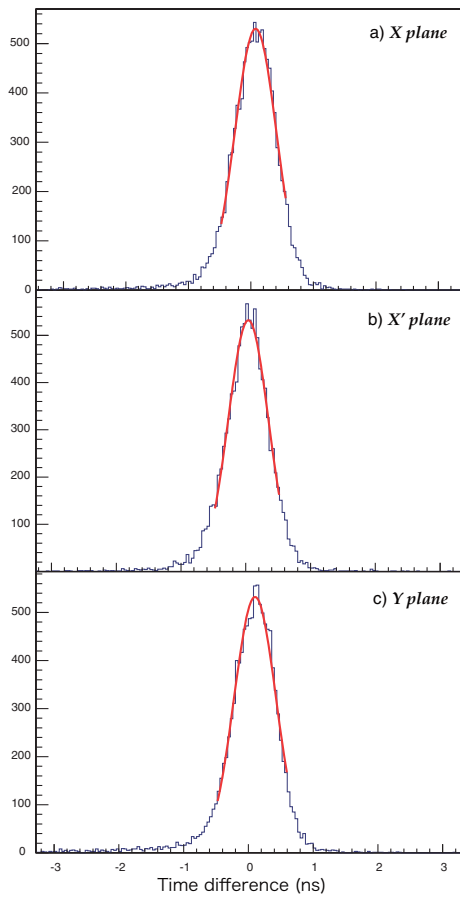


Fig. 7 Time difference between the timings recorded by the planes and that by VH. The widths obtained by fitting the curves show the time resolution of the detector. Peaks are broadened by the finite timing resolution of the VH counter.

The peaks are broadened with the uncertainty of the timing of VH. The width after removing quadratically the contribution of the VH resolution is also shown in the Table 1.

In addition, one can estimate the time resolution comparing the timing of a particle recorded by two of the planes. Fig. 8 shows the result. Fig. 8a, 8b, 8c show respectively the “time of flight” between X and X' planes, X and Y planes, and X' and Y planes. Here, the term “time of flight” is used, but in reality, this contains a certain arbitrary bias constant. The RMS width found by fitting these peaks are shown in Table 2. Now, assuming that the resolution of the “start” and “stop” planes are the same, one can evaluate the timing resolution by dividing these values by square root of two. These obtained resolutions are also shown in Table 2.

The resolution deduced from X and X' planes is observed to be smaller than others. The simple definition of the timing of one slab used in this analysis still might contain the dependence of the hit position within a slab. The hit positions within a slab in X and X' planes are similar, and thus the smallness of the resolution

of the X and X' might be explained by this effect.

Table 2 Evaluated timing resolution using the “time of flights” between two planes

planes used	RMS width of the peaks	estimated timing resolution
X – X'	377.4 ps	266.9 ps
X – Y	393.4 ps	278.1 ps
X' – Y	385.4 ps	272.5 ps

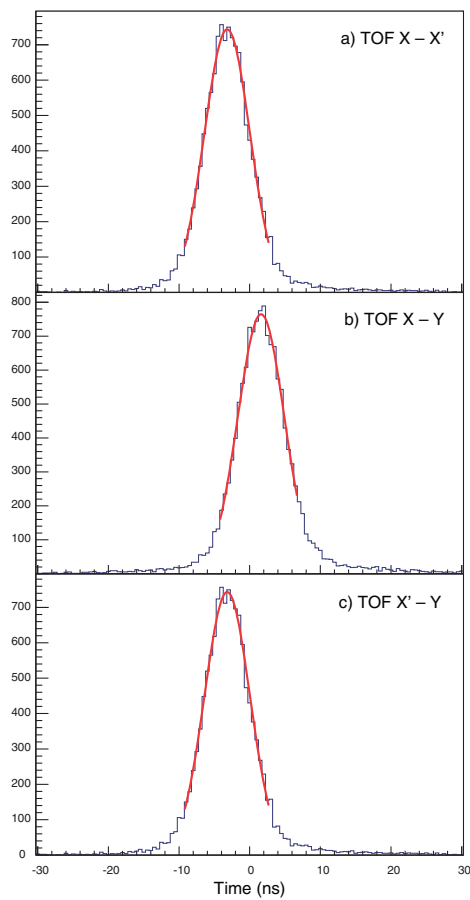


Fig. 8 The “time of flight (including an arbitrary constant)” between X and X' planes, X and Y planes, and X' and Y planes are shown respectively in (a), (b) and (c). The RMS width of these peaks are: 331.7 ps, 309.1 ps and 323.2 ps.

4.3 Detection efficiency

This counter is designed to be used in a high-intensity beam, and the real efficiency should be found out in a test using such a beam line. But as stated in the introduction, no such beam line was available at the time, the test was performed as described in the introduction.

Using the program Ariane, events with only one particle in each arm (positive and negative) of the DIRAC spectrometer are selected in the analysis. By tracing the particle in the positive arm, one chose the candidate events with a particle going through the window defined in chap. 4.1. Then on each plane of the detector the hits with a pulse height larger than the threshold of those candidate events are counted. Dividing the number of those events by the number of the candidate events, one could obtain the efficiency of each plane.

Table 3 shows the result of the efficiency evaluation carried out this way for the 3 planes tested in the first configuration.

Table 3 Evaluated detection efficiency of all the event

plane	hit on the plane	candidates	efficiency	threshold
X	10105	10320	0.978	740 channel
X'	9968	10329	0.965	745 channel
Y	9996	10329	0.968	745 channel

A higher efficiency was obtained when only events with e^+e^- trigger were used. The result is shown in Table 4.

Table 4 Evaluated detection efficiency of all the e^+e^- trigger events

plane	hit on the plane	candidates	efficiency	threshold
X	1015	1020	1.00	740 channel
X'	1013	1020	0.99	745 channel
Y	1011	1020	0.99	745 channel

It was found that the efficiencies obtained are better with e^+e^- trigger events. This is probably due to the fact that the divergence of the positrons going through the counter is smaller than that of the pions.

On the other hand, using the candidate events, we try to deduce the efficiency of each plane in using the number of coincident events between two planes and that of single hit events detected by one plane. The pulse-height of the hits must exceed the thresholds set on each plane. By dividing the former by the latter, one can evaluate the detection efficiency of a plane.

The results are shown in Table 5.

Table 5 Evaluated detection efficiency using two planes

plane	normalized with	efficiency	normalized with	efficiency
X	X'	0.997	Y	0.993
X'	Y	0.985	X	0.984
Y	X	0.982	X'	0.988

We also performed the same evaluation with e^+e^- trigger events. The results are presented in Table 6. The efficiency is apparently a little better in the former case using all the triggers.

Table 6 Evaluated detection efficiency of the e^+e^- events using two planes

plane	normalized with	efficiency	normalized with	efficiency
X	X'	1.00	Y	1.00
X'	Y	0.99	X	0.99
Y	X	0.99	X'	0.99

5. Discussion and conclusions

Although this counter is aimed at being used in a very high-intensity beam, no such beam line was available for the test. The counter was placed among the backward counters in the DIRAC spectrometer.

At the time of the test, only 6 units of F1-TDC-ADC were available. Thus by changing the instrumented planes in turn in 4 configurations, we tested the whole detector. A test with the counter fully instrumented was performed using the cosmic ray, and the result is reported in [3].

The F1-TDC-ADC allows to record the timing and the pulse height at the same time. This is ideal to examine in detail the nature of each hit, quite suitable for an experiment such as DIRAC where the meaningful events are very rare. The disadvantage, however, of the unit is that the pulse height is not recorded for hits with very small pulse height. That means the so-called pedestal is missing in the pulse-height spectra. Should one sees the pedestal, from its position together with the information about the position of the single-photoelectron peak, one would easily evaluate the number of photoelectrons in the minimum-ionizing peak assuming the linearity of the PMT response. For that reason, the absolute value of the number of photoelectrons obtained in the passage of a minimum-ionizing particle, which is strongly related to the efficiency of the counter was not seen in this study. A more traditional ADC was used in the test [3] using the cosmic ray and one could find the information concerning the absolute amount of light obtained.

We acknowledge the kindness of DIRAC collaboration who allowed to make a test in the DIRAC spectrometer. Also a lot of technical support has been provided by the members of the collaboration.

References

- [1] B. Adeva et al., Detection of $p^+ p^-$ atoms with the DIRAC spectrometer at CERN, *Journal of Physics G* **30** (2004) 1929-1946;
B. Adeva et al., Determination of $\pi^+ \pi^-$ scattering lengths from measurement of $\pi^+ \pi^-$ atom life, *Phys. Letters B* **704** (2011) 24, and the references therein
- [2] F. Takeutchi, Evaluation of the new dE/dx counter (new IH) prototype for the DIRAC experiment at CERN PS, *Bull. Res. Inst. of Adv. Tech, Kyoto Sangyo University* **IX** 2010
- [3] 青垣総一郎, 岡田憲志, 竹内富士雄, CERN PSにおける DIRAC 実験 (PS212) 用 dE/dx 検出器の宇宙線を用いた性能評価, To be published in *Bull. Res. Inst. of Adv. Tech, Kyoto Sangyo University*; New dE/dx counter 製作指針と構造 / 京産大での実験と結果, Sept. 11, 2012.
- [4] F. Takeutchi and S. Horikawa, Read-out using F1-TDC-ADC of the newSFD X plane (and dE/dx counter),

Bull. Res. Inst. of Adv. Tech, Kyoto Sangyo University **VII** 2008

- [5] A. Gorin et al., High resolution scintillating-fibre hodoscope and its readout using Peak-sensing algorithm, Nucl. Instr. Meth. in Phys. Res. **A 566** (2006) 500-515
- [6] P. Doskarova, private communication
- [7] <http://dirac.web.cern.ch/DIRAC/offlinedocs/Userguide.html>

DIRAC 実験ビームコースを使った new dE/dx 検出器の性能試験

青 垣 総一郎
千 葉 雅 美
岡 田 憲 志
竹 内 富士雄

要 旨

CERN の PS で行っている DIRAC 実験の第二ステージでは $\pi^+\pi^-$ 原子の Lamb-shift を測定するため強いビーム強度が要求される。そこで、高強度のビーム下で使用できる新しい dE/dx 検出器を設計・製作した。性能試験は DIRAC スペクトロメータのラインの中にこの検出器を設置して行った。その結果、検出効率や時間分解能に関して非常に良い性能が得られた。この計測の前に、宇宙線を使った光量に関する性能試験を京都産業大学の実験室で行ったが、その結果はこの冊子の別の論文に掲載している。

キーワード：DIRAC 実験、 $\pi^+\pi^-$ 原子、dE/dx ホドスコープ、位置検出型光電子増倍管、ファイバーライトガイド